

Towards a bio-inspired burrowing robot: Influence of the tip shape for soil vertical penetration

Ilya Brodoline^{1*}, Floriana Anselmucci¹, Hongyang Cheng¹, Ali Sadeghi² and Vanessa Magnanimo¹

¹ University of Twente, Chair of Soil Micro Mechanics, Faculty of Engineering Technology, MESA+, Drienerlolaan 5, 7522 NB, Enschede, The Netherlands.

² University of Twente, Soft Robotics Lab, Department of Biomedical Engineering, Faculty of Engineering Technology, Drienerlolaan 5, 7522 NB Enschede, The Netherlands.

*Corresponding author: i.b.brodoline@utwente.nl

ABSTRACT

This research exploits biomimicry to engineer innovative solutions for soil exploration and tunnelling in complex environments where soil burrowing is the main challenge. Drawing inspiration from the effective burrowing mechanisms of earthworms, we focused on the development of a untethered bio-inspired earthworm-like robot that faithfully replicates the morphology and behavior of *Lumbricus terrestris*. While prior efforts have primarily explored the horizontal soil burrowing using small diameter probes, in this study we focused on the vertical burrowing capability of a 30 mm diameter robot body. We conducted an experimental parametric analysis of multiple robot's tip shapes, concentrating on dry sand as the singular soil type. We inserted each tip at a constant speed and monitored the vertical force magnitude depending on the penetration depth. Higher aspect ratios showed better performance, reducing the penetration force compared to low ratios. Experiments showed that asymmetric tips, designed to enhance horizontal locomotion, do not compromise their performance in vertical burrowing. Additionally, we investigated soil fluidization through pressurized air, that effectively reduced shear resistance and facilitated tip penetration by up to 27%. These findings provide valuable insights into the forces requirements for penetrating deeper soil layers, and are essential for accurately design burrowing robots.

Keywords: Bio-inspiration; biomimicry; soil penetration; experimental investigation; tip shape; aspect ratio.

1. Background and Motivation

The pressing need to address climate change, with the imperative shift toward cleaner energy sources, is driving researchers to seek innovative engineering solutions in highly energy intensive processes, like soil exploration, utility deployment, and tunneling.

Nature, with its rich repertoire of solutions, becomes an inspiring source for crafting effective and minimally invasive engineering technologies. Over the past decades, researchers in geotechnical engineering have proposed different bio-inspired solutions. The mimic of mussels' fibers has shown promising potential in enhancing the adhesive performance of soil, rock, and concrete [Zhang et al., 2023]. Sangadji and Schlangen [Sangadji and Schlangen, 2013] replicated the femur's material properties and healing process to develop a novel approach to create a self-healing process for porous concrete cylinders. Finally [Martinez and O'Hara, 2021] showed that the anisotropic friction properties of snakeskin is an optimal design to increase the shaft resistance, proposing a new foundation concept in geotechnical engineering.

Previous advances in artificial burrowing, especially in the robotic communities, have highlighted the potential of biomimicry in addressing soil penetration challenges. [Rafsanjani et al., 2018] showed that the kirigami principles can be exploited to create bio-inspired flexible skins with directional frictional properties that can be integrated in soft robots to achieve locomotion even with a single extending actuator. [Sadeghi et al., 2014] showed a pioneering work, presenting a burrowing device inspired by the plant root

penetration technique. [Borela et al., 2021, Das et al., 2023] showed how earthworm-inspired peristaltic movement can be an ideal solution to design new burrowing devices.

The presented research consolidates the burrowing ability of earthworms [Francis et al., 2001] to develop a new bio-inspired burrowing soft robot for soil investigation. Through evolution, earthworms have perfected the art of burrowing, showcasing nature's ingenuity in solving complex locomotion challenges [Martinez et al., 2022]. Their highly energy-efficient peristaltic motion, combining anchoring and advancement-penetration, offers promise for the development of innovative, minimally invasive technologies. In Figure 1, a single crawling sequence of our preliminary pneumatic earthworm-like robot prototype is shown. The motion of the robot can be decomposed into three steps. The movement starts with the anchorage of the tail into the ground by inflating the rear chamber. Then, the elongation of the robot is achieved by inflating the longitudinal core chamber, generating enough force to penetrate the soil. Lastly, the body is moved forwards by anchoring the tip chamber then deflating the tail and the core. The challenge of this locomotion is to be able to generate enough force to penetrate the soil horizontally and vertically until the desired depth. Additionally, the robot has to overcome the rotation forces acting during underground steering.

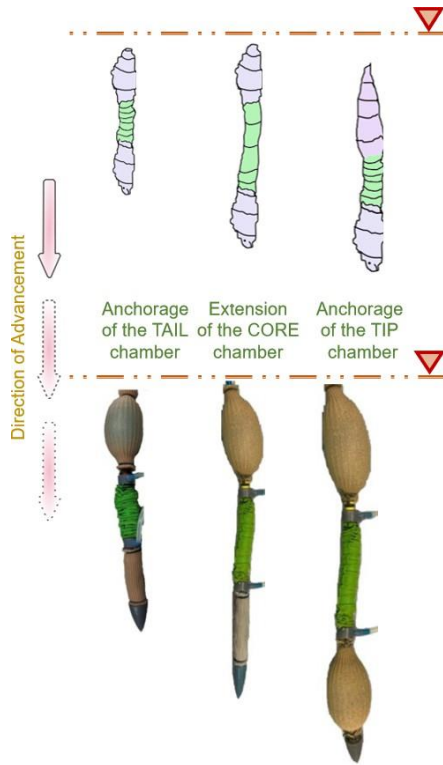


Figure 1. Prototype of a three-chambered earthworm-like borrowing robot.

Our work seeks to contribute to the understanding of the importance of the probe tip shape and penetration techniques during vertical burrowing. This paper will focus solely on the forces exerted at the interaction between the robot and soil at the tip, setting aside the challenge of anchoring and steering.

First, we investigated the potential impact of tip shapes on the burrowing process in terms of aspect ratio (AR), which has already proven its significance in drag reduction in the field of aeronautics [Stoney, 1954]. Secondly, we analyzed the effects of asymmetric geometry on vertical penetration forces, considering asymmetry demonstrated its efficiency for horizontal burrowing [Patino-Ramirez and O’Sullivan, 2024]. Finally, we analyzed the impact of soil fluidization through air injection.

2. Methodology and experimental investigation

2.1. Experimental setup

Experiments were conducted in a controlled environment using a cylindrical tank filled with dry sand. The dimensions of the tank were as follows: diameter - 24 cm, height - 75 cm. The sand in the tank had a mean diameter $D_{50} = 0.4 \text{ mm}$ and its uniformity was characterized by a coefficient of uniformity C_u of 2, ($C_u = D_{60}/D_{10}$) indicating a uniform sand distribution. The dry friction angle ϕ of the soil is 39° . The soil bulk density was always maintained at approximately $1.10 \text{ g} \cdot \text{cm}^{-3}$, which indicated a very loose sand.

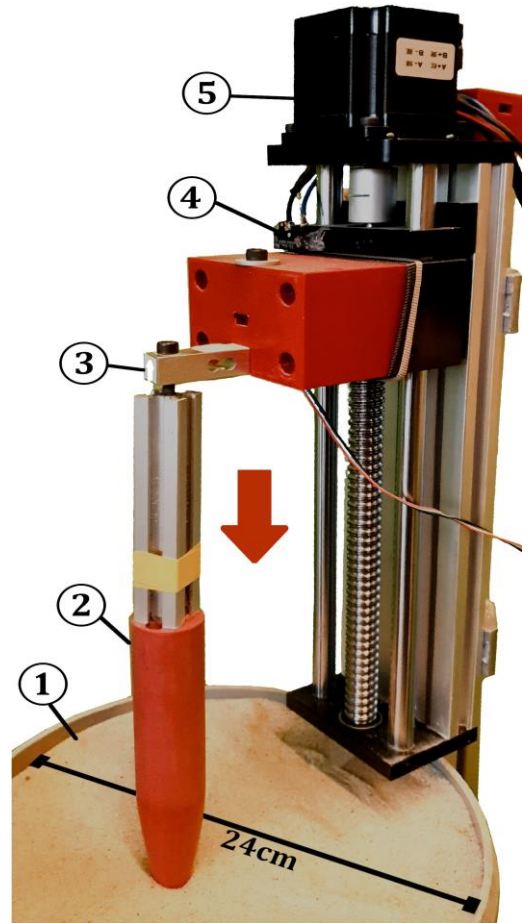


Figure 2. Photography of the experimental setup. (1) Penetration medium consisting of a tank of dry sand. (2) Tested 3D-printed probe. (3) Load cell. (4) Limit switch. (5) Stepper motor controlling the vertical position of the probe through a lead screw.

Five different probes were designed, and 3D printed using a polylactic acid thermoplastic polymer (PLA). Filled with a 10% grid pattern, the probes had an average mass of $25 \pm 5 \text{ g}$. Their surface was sanded up to a grit of 600. Each of them was tested separately in the controlled setup. As illustrated in Figure 2, to simulate the robot’s tip penetration, a rigid aluminum frame surrounding the cylindrical tank (1) was employed. The 3D-printed probe (2), with a body length of 170 mm, was attached to an aluminum profile (20×20×100 mm) screwed to the load cell (3), which was measuring the vertical penetration force of the probe. The load cell can sense a linear force up to 392 N. Probe immersion into the sand was controlled by the stepper motor (5), which operates the position of a vertical moving stage through a lead gear, with a maximum travel distance of 200 mm. The whole mechanical assembly was protected from dust by a fabric.


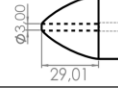
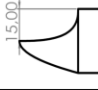


	Configuration	D [mm]	L [mm]	Aspect ratio (AR) (L / D)
AR _{1S}		30	30	1
AR _{1F}		30	30	1
AR _{1A}		30	30	1
AR _{2.5S}		30	75	2.5
AR _{4S}		30	120	4

Figure 3. Table of tested tip shapes.

Figure 3 presents the five distinct robot tips tested. Each differs in the aspect ratio (AR) or in the tip geometry. The tips are extended by a cylindrical body to keep the total length of each probe constant. A total of 3 different AR were tested. The AR is defined as the ratio between the tip length (L) and the tip diameter (D) [Stoney, 1954]. This parameter allowed us to establish a correlation between the geometry of the probe tip and the force required for penetration. For all the tips, the shape is following the typical Von Kármán nose type, defined by the Equation 1 [Stoney, 1954].

$$\theta(x) = \cos^{-1}(1 - 2x/L)$$

$$y(x) = \frac{D}{2\sqrt{\pi}} \cdot \sqrt{\theta(x) - \frac{\sin(2\theta)}{2}} \quad (1)$$

Where $x \in [0, L]$ and $y \in [0, D/2]$ correspond to the horizontal and vertical coordinate of any point on the tip surface, respectively.

Furthermore, for the $AR = 1$, penetration tests were performed also with an additional fluidization system at the tip. The tip AR_{1F}, with a central channel of 3 mm, was connected to an air pump capable of inducing fluidization in the soil under an average airflow of $8 L \cdot \text{min}^{-1}$. Additionally, for the same $AR = 1$, an asymmetrical tip shape AR_{1A} was tested.

2.2. Experimental Data Acquisition and Penetration Measurements

For each test, the experimental setup allowed the systematic variation of penetrating depth at a constant speed of $5 \text{ mm} \cdot \text{s}^{-1}$.

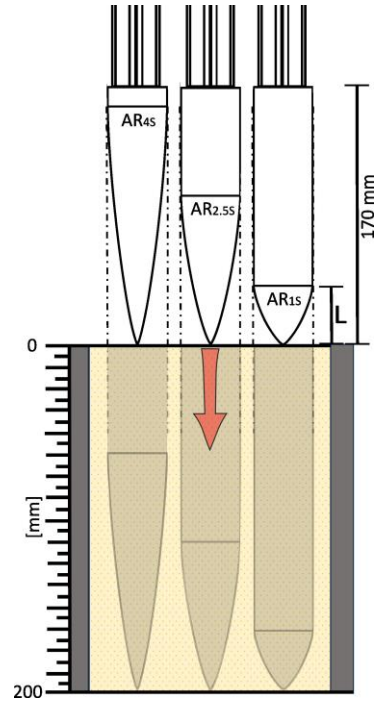


Figure 4. Scheme of the experimental setup for three different tip configurations penetrating into the tank of sand.

For each tip configuration (Figure 3), forces versus displacement were recorded every 1.25 mm using a 24-bit HX711 Analog-to-Digital converter running at 80 Hz. The force sensing and steps advancement was synchronized by an Arduino Uno R3 microcontroller connected to a HY-DIV268N-5A stepper motor driver. The initial position of the penetration probe was reset for every test through the use of a limit switch (denoted (4) in Figure 2).

In Figure 4, we illustrate the experimental procedure. The initial zero-position of each probe corresponds to the contact of the extremity with the soil surface. Then, the probes are inserted in the sand for 200 mm. Prior to each repetition, the soil was removed and reposed to always restore the same free-surface level and bulk density of $1.10 \text{ g} \cdot \text{cm}^{-3}$. This meticulous preparation ensured consistent soil conditions across tests. To enhance result accuracy and reliability, each test configuration was repeated at least four times, to capture any variability in experimental conditions.

3. Results

In this study we first investigated the influence of the Aspect Ratio (AR) on the penetration force needed in dry soil. For each of the investigated tip configuration, the vertical penetration force was measured through a load cell. The maximum depth reached is 200 mm . The results of the conducted experiments are presented in Figures 5, 6, and 7.

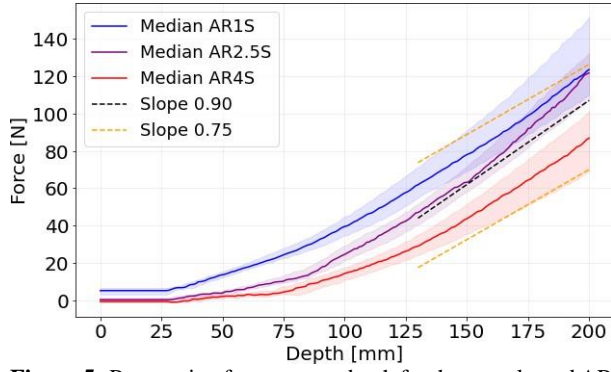


Figure 5. Penetration force versus depth for three evaluated AR of symmetric tips. For each measurement, the median curve is plotted over an area representing the minimum and maximum range of values observed across several repetitions (N). Dotted lines depict linear slopes, aiding in the interpretation of the results. $AR_{1S} : N = 10$, $AR_{2.5S} : N = 10$, $AR_{4S} : N = 10$.

In Figure 5, the penetration force relative to penetration depth is plotted for three AR of a symmetric tip: $AR = 1$, $AR = 2.5$, and $AR = 4$. The figure represents the data spread from repeated tests and highlights the median curve for each configuration. Linear slopes of 0.75 and 0.9 are included in the plot to aid the interpretation of the curves. Figure 5 shows that the tip with an AR of 4 has a consistently lower range of penetration forces compared to smaller AR values. Particularly, the ultimate force at a depth of 200 mm is 30% lower for $AR = 4$ than for $AR = 1$. This phenomenon likely results from the increased shear strain induced by this finer tip geometry, effectively reducing the force required for penetration.

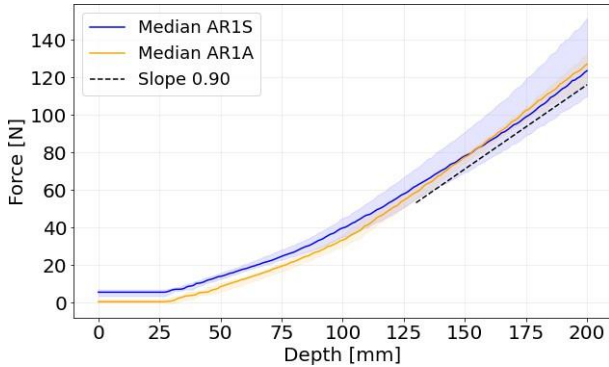


Figure 6. Penetration force versus depth to evaluate the influence of asymmetry in the tip with $AR = 1$. For each measurement, the median curve is plotted over an area representing the minimum and maximum range of values observed across several repetitions (N). Dotted line depicts linear slope, aiding in the interpretation of the results. For AR_{1S} , $N = 10$, for AR_{1A} , $N = 4$.

Following the comparative analysis across AR (Figure 5), we characterized the AR of 1 as exhibiting the highest penetration forces, and thus defined it as a reference. To understand how to improve the efficiency of this tip we subsequently investigated the impact of tip asymmetry and soil fluidization.

In Figure 6, the penetration force relative to penetration depth is plotted for the symmetrical tip AR_{1S} ,

compared to the asymmetrical tip AR_{1A} . While asymmetrical tip configuration displays slightly reduced data variability compared to the symmetrical tip, the median trends reveal that asymmetry has not a significant impact on the efficiency of vertical penetration. Both curves for penetrations higher than 120 mm have a constant slope of around 0.9. The penetration force is lower for the asymmetric geometry only under a depth of 75 mm, which could be due to uncertainties of shallow soil layers. Consequently, the similarity between the asymmetric AR_{1A} and the symmetric geometry AR_{1S} shows the possibility of using asymmetric robot tips known for reducing the drag and lift forces during horizontal burrowing [Patino-Ramirez and O’Sullivan, 2024], without having a significant impact on the vertical penetration force.

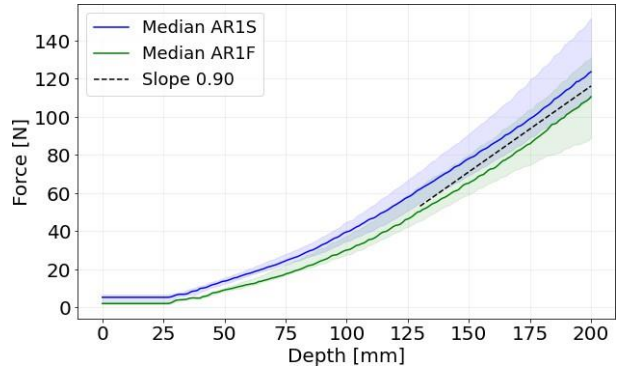


Figure 7. Penetration force versus depth to evaluate the influence of soil fluidization in the tip with $AR = 1$. For each measurement, the median curve is plotted over an area representing the minimum and maximum range of values observed across several repetitions (N). Dotted line depicts linear slope, aiding in the interpretation of the results. For AR_{1S} , $N = 10$, for AR_{1F} , $N = 4$.

Another strategy used to enhance soil burrowing is the soil fluidization. In our experiment, fluidization was achieved through the application of pressurized airflow at $8 L \cdot min^{-1}$ via a 3 mm diameter channel, mirroring techniques utilized in horizontal burrowing [Naclerio et al., 2021]. Figure 7 shows the comparison of the tip with fluidization AR_{1F} , with respect to the reference tip AR_{1S} . As depicted in Figure 7, fluidization effect is minimal at shallower depths under 80 mm. However, at deeper depths, fluidization significantly decreases penetration force by up to 27%, underscoring its potential to enhance penetration efficiency under this specific conditions. Also, in this case at higher depth, the slopes of the two curves remain constant at around 0.9, highlighting that the fluidization reduced the needed penetration force. Similar to findings reported by [Naclerio et al., 2021], our results suggest that soil fluidization presents a viable strategy for reducing vertical penetration forces, thereby enhancing the operational efficiency of robotic systems in soil environments.

4. Conclusions

Designing a robot that mimics the burrowing behavior of an earthworm for soil exploration is challenging since its actuators have to overcome high penetration forces during burrowing. By addressing the

necessity for vertical penetration in different soil environments, our research aims to provide valuable insights and contribute to the broader advancement of biomimetic engineering technologies for sustainable solutions in challenging terrains.

Similar to aircraft noses, the shape of the robot's tip seems to have a significant impact on the penetration and in reducing these forces. This study focused on comparing vertical penetration forces depending on the aspect ratio of the tip. Diverging from related studies, we opted for a large tip diameter of 30 mm, which represents an appropriate size for building untethered robots. Through the proposed experimental setup, we demonstrated the advantage of high aspect ratios for soil exploration. Additionally, we found that asymmetrical tip shapes do not constitute a disadvantage to the vertical penetration, while keeping the benefits they present for horizontal burrowing. Lastly, we analyzed the effect of fluidization of the sand, demonstrating that a small fluidization has a positive impact on reducing the penetration forces. Although further investigations need to be carried out to quantify the disruptiveness of this approach towards the soil properties and structures at further distance from the tip location.

In conclusion, this study gives an initial dataset for accurately designing untethered burrowing robots. Tested tip configurations encompassed variations in probe tip geometry, penetration forces, and the introduction of soil fluidization, providing a comprehensive understanding of the factors influencing the penetration process in diverse soil conditions. Next, this work will focus on completing the presented dataset, by exploring the horizontal penetration and underground bending. Friction components should also be investigated, to accurately identify its contribution to the measurements.

Acknowledgements

This publication is part of the project 'Bio-inspired burrowing robot for soil penetration in limited-access sites' with project number [15423] of the research programme [Open Competition Domain Science XS packet 22-4] which is (partly) financed by the Dutch Research Council (NWO). The authors would like to acknowledge funding from Crazy Idea initiative from the Faculty of Engineering Technology at University of Twente.

References

- [Borela et al., 2021] Borela, R., Frost, J., Viggiani, G., and Anselmucci, F. (2021). Earthworm-inspired robotic locomotion in sand: An experimental study with x-ray tomography. *Géotechnique Letters*, 11(1):66–73.
- [Das et al., 2023] Das, R., Babu, S. P. M., Visentin, F., Palagi, S., and Mazzolai, B. (2023). An earthworm-like modular soft robot for locomotion in multi-terrain environments. *Scientific Reports*, 13(1):1571.
- [Francis et al., 2001] Francis, G., Tabley, F., Butler, R., and Fraser, P. (2001). The burrowing characteristics of three common earthworm species. *Soil Research*, 39(6):1453–1465.
- [Martinez et al., 2022] Martinez, A., DeJong, J., Akin, I., Aleali, A., Arson, C., Atkinson, J., Bandini, P., Baser, T., Borela, R., Boulanger, R., et al. (2022). Bio-inspired geotechnical engineering: Principles, current work, opportunities and challenges. *Géotechnique*, 72(8):687–705.
- [Martinez and O'Hara, 2021] Martinez, A. and O'Hara, K. (2021). Skin friction directionality in monotonically and cyclically-loaded bio-inspired piles in sand. *Deep Found. Inst. J*, 15(1):1–15.
- [Naclerio et al., 2021] Naclerio, N. D., Karsai, A., Murray-Cooper, M., Ozkan-Aydin, Y., Aydin, E., Goldman, D. I., and Hawkes, E. W. (2021). Controlling subterranean forces enables a fast, steerable, burrowing soft robot. *Science Robotics*, 6(55):eabe2922.
- [Patino-Ramirez and O'Sullivan, 2024] Patino-Ramirez, F. and O'Sullivan, C. (2024). Optimal tip shape for minimum drag and lift during horizontal penetration in granular media. *Acta Geotechnica*, 19(1):19–38.
- [Rafsanjani et al., 2018] Rafsanjani, A., Zhang, Y., Liu, B., Rubinstein, S. M., and Bertoldi, K. (2018). Kirigami skins make a simple soft actuator crawl. *Science Robotics*, 3(15):eaar7555.
- [Sadeghi et al., 2014] Sadeghi, A., Tonazzini, A., Popova, L., and Mazzolai, B. (2014). A novel growing device inspired by plant root soil penetration behaviors. *PLoS one*, 9(2):e90139.
- [Sangadji and Schlangen, 2013] Sangadji, S. and Schlangen, E. (2013). Mimicking bone healing process to self repair concrete structure novel approach using porous network concrete. *Procedia Engineering*, 54:315–326.
- [Stoney, 1954] Stoney, W. E. (1954). Transonic Drag Measurements of Eight Body-nose Shapes. *National Advisory Committee for Aeronautics - No. NACA-RM-L53K17*, (NACA-RM-L53K17).
- [Zhang et al., 2023] Zhang, W., Xiang, J., Huang, R., and Liu, H. (2023). A review of bio-inspired geotechnics-perspectives from geomaterials, geocomponents, and drilling & excavation strategies. *Biogeotechnics*, 1(3):100025.